J Electroceram (2006) 17:231–234
DOI 10.1007/s10832-006-6994-9

Sapphire orientation dependence of the microstructure of ZnO thin film during annealing

Tae Sik Cho · Min-Su Yi · Ji Wook Jeung · Do Young Noh · Jin Woo Kim · Jung Ho Je

Received: 26 June 2005 / Revised: 11 October 2005 / Accepted: 23 December 2005

Abstract The sapphire orientation dependence of the microstructure of ZnO thin films has been studied in real-time synchrotron X-ray scattering experiments. The ZnO films with a 2400-Å-thick were grown on sapphire (001) and sapphire (110) substrates at room temperature by radio frequency magnetron sputtering. The as-deposited ZnO film on sapphire (001) has the only (002) crystal grains, while that on sapphire (110) has not only (002) crystal grains but (100) and (101) additional grains. The ZnO films were changed into fully epitaxial ZnO (002) grains both on sapphire (001) and sapphire (110) substrates with increasing the annealing temperature to 600°C. The epitaxial relationships of the ZnO grains were summarized as ZnO (00*l*)[100]//sapphire (00*l*)[110] and ZnO (00*l*)[110]//sapphire (110)[001].

Keywords ZnO thin film · Sapphire orientation · Synchrotron X-ray scattering · Annealing

1 Introduction

In recent years, wide band gap semiconductor materials such as ZnO and GaN have attracted much attention for the development of blue light emitting diodes and laser diodes. In particular, ZnO has some notable properties of the large bond strength and the extreme stability of excitons, offering the prospect of the practical lasers with low thresholds even at high temperature [1, 2]. But defects of the ZnO thin films degrade efficient and lasting emission [3]. In connection with this, it is important to investigate the microstructure and the thermal stability of ZnO thin films during real-time annealing.

In this paper, we present real-time synchrotron X-ray scattering study of the sapphire orientation dependence of the microstructure of ZnO thin films during annealing. Our study reveals that the ZnO thin films were changed into fully epitaxial ZnO (002) grains both on sapphire (001) and sapphire (110) substrates with increasing the annealing temperature to 600°C. The epitaxial relationships of the ZnO grains were summarized as ZnO (00*l*)[100]//sapphire (00*l*)[110] and ZnO (00*l*)[110]//sapphire (110)[001].

2 Experimental

The ZnO thin films were grown on sapphire (001) and sapphire (110) substrates at room temperature by radio frequency (rf) magnetron sputtering of a stoichiometric ZnO target. As a carrier gas, a mixture of Ar-10% O_2 was used. The rf power was 1 W/cm^2. The deposition rate of the film was about 2 Å/min. The thickness of the as-deposited film studied in this experiment, determined by X-ray reflectivity measurement [4], was 2400 Å.

The synchrotron X-ray scattering experiments were performed at beamline 5C2 (GIST) at Pohang Light Source (PLS) in Korea. The incident X-rays were vertically focused by a mirror, and monochromatized to the wavelength of 1.333 Å by a double bounce Si (111) monochromator.

T.S. Cho (✉)· M.-S. Yi · J.W. Jeung
Department of Materials Science and Engineering, Sangju National University, Sangju, Kyungbuk, 742-711, Korea
e-mail: tscho@sangju.ac.kr

D.Y. Noh · J.W. Kim
Department of Materials Science and Engineering, Gwangju Institute Science and Technology, Gwangju, 506-712, Korea

J.H. Je
Department of Materials Science and Engineering and Center for Information Materials, Pohang University of Science and Technology, Pohang, Kyungbuk, 790-784, Korea

The as-deposited film was annealed to 600°C in air using a small heating stage, which was set on a four-circle X-ray diffractometer for the real-time X-ray measurements. The temperature was raised step by step and kept constant during the X-ray scattering measurements.

3 Results and discussion

We first discuss the annealing behavior of ZnO thin films with a 2400-Å-thick grown both on sapphire (001) and sapphire (110) substrates at room temperature. Figure 1 shows a series of powder X-ray diffraction profiles of ZnO thin films obtained during real-time annealing in air at several temperatures. At room temperature, there exists a strong Bragg reflection at near the $q_z = 2.414$ Å^{-1}, corresponding to the ZnO (002) grains both on sapphire (001) and sapphire (110) substrates (JCPDS 36-1451). The growth behavior is a general trend irrespective of growth conditions, as previously reported [5]. As we examined the details of the diffraction data, we noticed that the as-deposited ZnO film on sapphire (001) has the only (002) Bragg reflection, while that on sapphire (110) has not only (002) Bragg reflection but also additional, small, Bragg reflections at $q_z = 2.220$ and $q_z = 2.525$ Å^{-1} that correspond to the ZnO (100) and ZnO (101) reflections, respectively.

As shown in Fig. 1(a), the only (002) Bragg reflection of the ZnO film on sapphire (001) became gradually symmetric with increasing the annealing temperature. This was originated from the strain relaxation of the film with the annealing temperature [6, 7]. The lattice strain at room temperature is large as 0.35%, while that at 600°C is small as 0.10%. As illustrated in Fig. 1(b), the additional (100) and (101) Bragg reflection of the ZnO film on sapphire (110) gradually decreased and disappeared with increasing the annealing temperature, while the (002) Bragg reflection increased indicating that the (002) grains grows further by recrystallization. The lattice strain at room temperature is very large as 0.62%, while that at 600°C is small as 0.11%. With increasing the annealing temperature to 600°C, the ZnO thin films were changed into fully ZnO (002) grains both on sapphire (001) and sapphire (110) substrates.

In order to study the epitaxial relationship, we need to observe additional Bragg reflections in nonspecular directions [8]. Figure 2(a) and (b) show the scattering intensity profiles of the nonspecular ZnO (101) reflections on the azimuthal

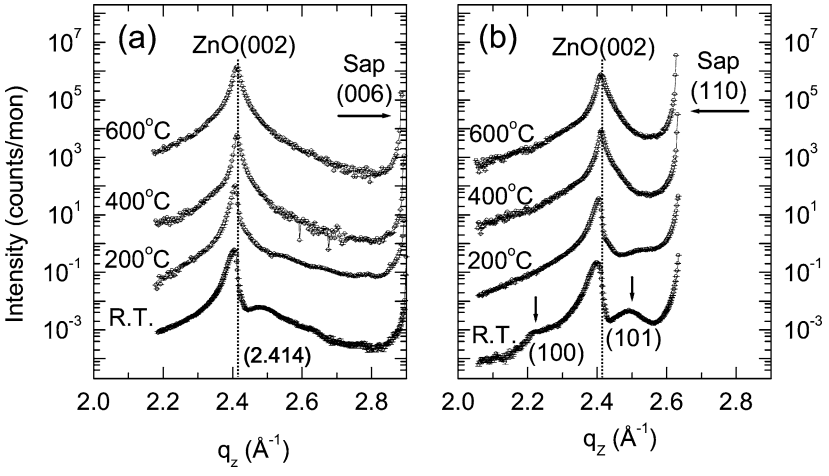

Fig. 1 X-ray powder diffraction profiles of ZnO thin films grown on (a) sapphire (001) and (b) sapphire (110) substrates, measured at several temperatures during real-time annealing

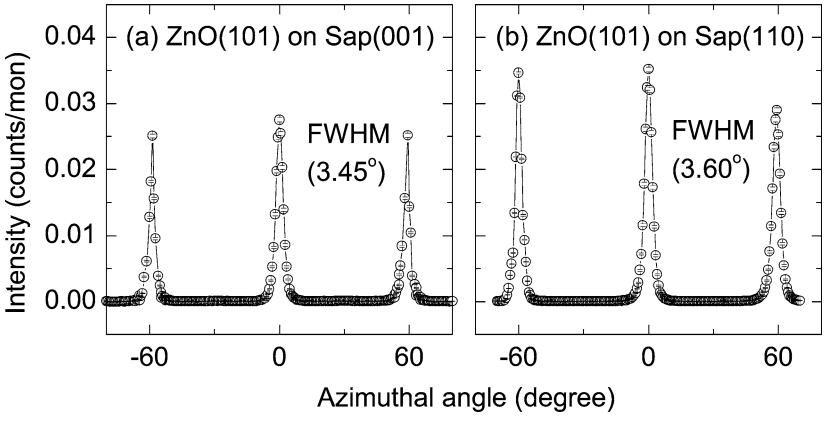

Fig. 2 X-ray intensity profiles of the nonspecular ZnO (101) reflections on (a) sapphire (001) and (b) sapphire (110) substrates

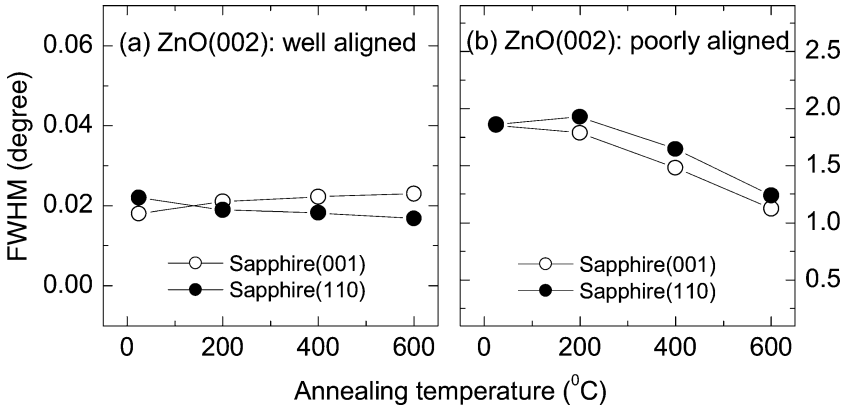

Fig. 3 FWHMs in the θ-rocking curve of Bragg reflection of (a) the well aligned ZnO (002) grains and (b) the badly aligned ZnO (002) grains, grown on sapphire (001) and sapphire (110) substrates, measured at several temperatures during real-time annealing

circle of the films grown both on sapphire (001) and sapphire (110) substrates, respectively. The sharp scattering features with six-fold symmetry show that the ZnO grains were grown epitaxially both on sapphire (001) and sapphire (110) substrates. The distributions of the in-plane crystalline axis of the ZnO grains was sharply peaked with the full width at half maximums (FWHMs) of 3.45° and 3.60° on sapphire (001) and sapphire (110) substrates, respectively. In the ZnO/sapphire (001) film, ZnO oxygen atoms would bond to the underlying sapphire Al atoms to form a structure with a mismatch of 31.8% [9]. In the meanwhile, the sapphire (110) surface is twofold symmetric, while the ZnO (002) surface is sixfold symmetric; the two surfaces are essentially incommensurate with the exception that the ZnO [110] and the sapphire [001] are related almost exactly by a factor of 4 (mismatch less than 0.08%) [9]. The epitaxial relationships of the ZnO grains were summarized as ZnO (00*l*)[100]//sapphire (00*l*)[110] and ZnO (00*l*)[110]//sapphire (110)[001], as previously reported [9].

The mosaic distribution, which is usually studied by measuring the FWHM in the theta (θ)-rocking curve of Bragg reflection, represents the epitaxial quality of a thin film [10, 11]. The mosaic distribution of the as-deposited ZnO films with a 2400-Å-thick was composed of the sharp and the broad components with about 0.02° and 1.86° FWHMs, respectively (data not shown). We believe that the broad component is originated from the 3D islands that are nucleated, as poorly aligned grains, on the well aligned (sharp component), highly strained, 2D layers grown in the initial stage [12].

To illustrate the amount of ZnO phase quantitatively [13], the X-ray integrate intensities was obtained by integrating the diffraction signal in the rocking curves of (002) reflections of the as-deposited ZnO films with a 2400-Å-thick. The amount of the poorly aligned ZnO (002) grains was very much at 0.50–0.58, compared to that of the well aligned grains, 0.015–0.017 (arbitrary unit). This result immediately indicated that the poorly aligned (002) grains were mostly occupied as major grains in the ZnO films.

Figure 3 shows the FWHMs of (a) the well aligned and (b) the poorly aligned ZnO (002) grains, grown on sapphire (001) and sapphire (110) substrates, measured at several temperatures during real-time annealing. With increasing the annealing temperature to 600°C, we note that the mosaic distribution of the well aligned ZnO (002) grains remained constant as about 0.02° FWHM, while that of the poorly aligned ZnO (002) grains decreased regardless of sapphire substrates. This result clearly indicated that the epitaxial crystal quality of the ZnO films, grown on sapphire (001) and sapphire (110) substrates, was improved with increasing the annealing temperature.

We estimate the crystal domain size (CDS) of the well aligned and the poorly aligned ZnO (002) epitaxial grains in

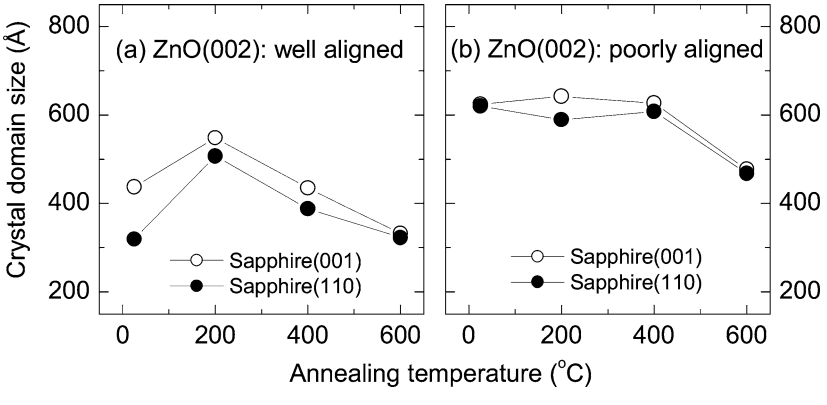

Fig. 4 Crystal domain sizes of (a) the well aligned and (b) the badly aligned ZnO (002) grains, grown on sapphire (001) and sapphire (110) substrates, measured at several temperatures during real-time annealing

the film normal direction by the FWHM of the θ-2θ scattering profile using Sherrer's formula [11, 14]. Although the scattering profile is asymmetric, we can still use the width of the profile to estimate the given direction. Figure 4(a) shows the CDSs of the well aligned ZnO (002) grains, grown on sapphire (001) and sapphire (110) substrates, measured at several temperatures during real-time annealing. The CDSs of the well aligned ZnO (002) grains reached to a maximum at 200°C due to the defect annealing, and decreased gradually at temperatures above 200°C regardless of sapphire substrates. Figure 4(b) shows the CDSs of the poorly aligned ZnO (002) grains, grown on sapphire (001) and sapphire (110) substrates, with increasing the annealing temperature. We noted that the CDS of the poorly aligned grains remained constant to 400°C, and decreased at temperatures above 400°C regardless of sapphire substrates. This result indicated that the thermal stability of the ZnO (002) crystal grains was degraded at temperatures above 400°C.

4 Summary

We have studied the sapphire orientation dependence of the microstructure of ZnO thin films during real-time annealing to 600°C in air by synchrotron X-ray scattering. The ZnO thin films with a 2400-Å-thick were grown on sapphire (001) and sapphire (110) substrates at room temperature by rf magnetron sputtering. The as-deposited ZnO film grown on sapphire (001) has the only epitaxial (002) crystal grains, while that grown on sapphire (110) has not only epitaxial (002) crystal grains but also additional (100) and (101) polycrystal grains. The ZnO thin films were changed into fully epitaxial ZnO (002) grains both on sapphire (001) and sapphire (110) substrates with increasing the annealing temperature to 600°C. The crystal quality of ZnO film was also improved with annealing temperature, while the crystal domain size was decreased at temperatures above 400°C. The epitaxial relationships of the ZnO grains were summarized as ZnO (00*l*)[100]//sapphire (00*l*)[110] and ZnO (00*l*)[110]//sapphire (110)[001]. Further study is reguired to elucidate the detailed strain relaxations of (002) grains during the annealing of ZnO/sapphire films.

Acknowledgments This work was supported by grant No. (R05-2002-000-01186-0) from the Basic Research Program of the KOSEF. Experiments at PLS were also supported in part by MOST and POSTECH.

References

1. Z.K. Tang, G.K.L. Wong, P. Yu, M. Kawasaki, A. Ohtomo, H. Koinuma, and Y. Segawa, *Appl. Phys. Lett.*, **72**, 3270 (1998).
2. D.M. Bagnall, Y.F. Chen, Z. Zhu, T. Yao, M.Y. Shen, and T. Goto, *Appl. Phys. Lett.*, **73**, 1038 (1998).
3. R.F. Service, *Science*, **276**, 895 (1997).
4. D.Y. Noh, Y. Hwu, H.K. Kim, and M. Mong, *Phys. Rev., B*, **51**, 4441 (1995).
5. K.H. Kim, K.C. Park, and D.Y. Ma, *J. Appl. Phys.*, **81**, 7764 (1997).
6. H.C. Kang, S.H. Seo, and D.Y. Noh, *J. Mater. Res.*, **16**, 1814 (2001).
7. M.S. Yi and D.Y. Noh, *Appl. Phys. Lett.*, **78**, 2443 (2001).
8. T.S. Cho, S.J. Doh, J.H. Je, and D.Y. Noh, *Appl. Phys. Lett.*, **74**, 2050 (1999).
9. P. Fons, K. Iwata et al., *Appl. Phys. Lett.*, **77**, 1801 (2000).
10. T.S. Cho, S.J. Doh, J.H. Je, and D.Y. Noh, *J. Appl. Phys.*, **86**, 1958 (1999).
11. B.D. Cullity, *Elements of X-ray Diffraction* (Addison-Wesley, MA, 1978), Chap. 3.
12. S.I. Park, T.S. Cho, S.J. Doh, J.L. Lee, and J.H. Je, *Appl. Phys. Lett.*, **77**, 349 (2000).
13. T.S. Cho, J.H. Je, and D.Y. Noh, *Appl. Phys. Lett.*, **76**, 303 (2000).
14. B.E. Warren, *X-ray Diffraction* (Addison-Wesley, MA, 1969), Chap. 14.